POLITECNICO DI TORINO
Repository ISTITUZIONALE

Dewatering of Scenedesmus Obliquus Cultivation Substrate with Microfiltration: Potential and Challenges for Water Reuse and Effective Harvesting

Original
Dewatering of Scenedesmus Obliquus Cultivation Substrate with Microfiltration: Potential and Challenges for Water Reuse and Effective Harvesting / Malaguti, Marco; Craveri, Lorenzo; Ricceri, Francesco; Riggio, Vincenzo; Zanetti, Mariachiara; Tiraferri, Alberto. - In: ENGINEERING. - ISSN 2095-8099. - 38:(2024), pp. 155-163. [10.1016/j.eng.2023.07.010]

Availability:
This version is available at: 11583/2991791 since: 2024-08-19T17:16:21Z

Publisher:
Elsevier

Published
DOI:10.1016/j.eng.2023.07.010

Terms of use:

This article is made available under terms and conditions as specified in the corresponding bibliographic description in the repository

Publisher copyright
Elsevier postprint/Author's Accepted Manuscript

© 2024. This manuscript version is made available under the CC-BY-NC-ND 4.0 license http://creativecommons.org/licenses/by-nc-nd/4.0/.The final authenticated version is available online at: http://dx.doi.org/10.1016/j.eng.2023.07.010

(Article begins on next page)

08 May 2026

Engineering 38 (2024) 155–163

Contents lists available at ScienceDirect

Engineering

journal homepage: www.elsevier.com/locate/eng

Research
Environmental Sustainability—Article

Dewatering of *Scenedesmus obliquus* Cultivation Substrate with Microfiltration: Potential and Challenges for Water Reuse and Effective Harvesting

Marco Malaguti [a], Lorenzo Craveri [a], Francesco Ricceri [a,b], Vincenzo Riggio [a], Mariachiara Zanetti [a], Alberto Tiraferri [a,b,*]

[a] *Department of Environment, Land and Infrastructure Engineering, Politecnico di Torino, Torino 10129, Italy*
[b] *Clean Water Center, Politecnico di Torino, Torino 10129, Italy*

ARTICLE INFO

Article history:
Received 13 February 2023
Revised 20 July 2023
Accepted 21 July 2023
Available online 29 August 2023

Keywords:
Scenedesmus obliquus
Microfiltration
Permeate reuse
Harvesting
Microalgae
Pilot-scale

ABSTRACT

In the microalgae harvesting process, which includes a step for dewatering the algal suspension, directly reusing extracted water *in situ* would decrease the freshwater footprint of cultivation systems. Among various algae harvesting techniques, membrane-based filtration has shown numerous advantages. This study evaluated the reuse of permeate streams derived from *Scenedesmus obliquus* (*S. obliquus*) biomass filtration under bench-scale and pilot-scale conditions. In particular, this study identified a series of challenges and mechanisms that influence the water reuse potential and the robustness of the membrane harvesting system. In a preliminary phase of this investigation, the health status of the initial biomass was found to have important implications for the harvesting performance and quality of the permeate stream to be reused; healthy biomass ensured better dewatering performance (i.e., higher water fluxes) and higher quality of the permeate water streams. A series of bench-scale filtration experiments with different combinations of cross-flow velocity and pressure values were performed to identify the operative conditions that would maximize water productivity. The selected conditions, 2.4 $m \cdot s^{-1}$ and 1.4 bar (1 bar = 10^5 Pa), respectively, were then applied to drive pilot-scale microfiltration tests to reuse the collected permeate as a new cultivation medium for *S. obliquus* growth in a pilot-scale photobioreactor. The investigation revealed key differences between the behavior of the membrane systems at the two scales (bench and pilot). It indicated the potential for beneficial reuse of the permeate stream as the pilot-scale experiments ensured high harvesting performance and growth rates of biomass in permeate water that were highly similar to those recorded in the ideal cultivation medium. Finally, different nutrient reintegration protocols were investigated, revealing that both macro- and micro-nutrient levels are critical for the success of the reuse approach.

© 2023 THE AUTHORS. Published by Elsevier LTD on behalf of Chinese Academy of Engineering and Higher Education Press Limited Company. This is an open access article under the CC BY-NC-ND license (http://creativecommons.org/licenses/by-nc-nd/4.0/).

1. Introduction

The cultivation of microalgae is gaining interest due to the plethora of applications in which this type of biomass can be exploited for commercial purposes [1]. Microalgae are grown and harvested for use in several industrial sectors, such as food [2,3], cosmetics [4,5], wastewater treatment [6,7], and for energy and environmental applications, such as biofuel production and CO_2 fixation [8–10]. Among the different types of biomass, microalgae are generally easy to cultivate, and some strains may even be grown in harsh environments, while many are grown in land-saving photobioreactor systems [11,12]. In particular, the algae *Scenedesmus obliquus* (*S. obliquus*) is particularly suitable for biofuel production [13] and CO_2 sequestration, as well as being versatile for wastewater treatment applications [14,15]. Moreover, *S. obliquus* algae tend to grow well in solutions reused from the harvesting process [16].

Directly reusing the cultivation water *in situ* would increase the competitiveness of the algae market, which is currently limited by excessive costs and the need for abundant freshwater. One of the main drawbacks of microalgae applications is the large volume of water required per unit of biomass product [17]. Freshwater is

* Corresponding author.
E-mail address: alberto.tiraferri@polito.it (A. Tiraferri).

https://doi.org/10.1016/j.eng.2023.07.010
2095-8099/© 2023 THE AUTHORS. Published by Elsevier LTD on behalf of Chinese Academy of Engineering and Higher Education Press Limited Company.
This is an open access article under the CC BY-NC-ND license (http://creativecommons.org/licenses/by-nc-nd/4.0/).

continuously replaced in the photobioreactors to support the biological functions and growth of the algae. The water requirements translate to high management and environmental costs, which are further increased due to the energy used for transportation and the continual input of nutrients that must be dissolved in fresh water to provide an optimal cultivation medium [18]. After cultivation, algae are typically dewatered prior to further dehydration steps and the extraction of the final product. Finally, the wastewater extracted during the dewatering phase of the harvesting process is typically discharged, with or without treatment. The harvesting process accounts for 20%–30% of the total microalgae production costs and ample margins for cost reduction exist [19].

Recently, membrane filtration was shown to be a suitable process for algae biomass harvesting [20], specifically in the first steps of dewatering. The advantages of using membranes include that the separation can be carried out continuously and that membranes are assembled in modules, thus providing flexibility and ease of scale-up and capacity adjustments [21]. Innovative membrane filtration experiments have been presented by Nedzerek et al. [22] and Discart et al. [23], who evaluated permeate recycling in a membrane photobioreactor with the algae *Chlorella vulgaris*. Promising results regarding the reuse potential of *S. obliquus* systems have been reported by Ricceri et al. [16], who identified an optimal membrane with an average pore size of 0.14 μm for energy-efficient harvesting. Notably, forward osmosis has also been shown to be effective in the dewatering of the *S. obliquus* strain [24]. However, direct water reuse of the draw solution is not possible because of the presence of the draw agent [25]. Past studies have mainly focused on bench-scale systems, and process scale-up still represents an important challenge [26–31]. Moreover, contradictory results have been reported, partly due to the complexity of biological microalgae systems and partly due to the lack of standardized practices. Furthermore, consideration of the mechanisms involved, such as the influence of the scale of operation or the intrinsic variability among batches of microalgae [32–34], has varied among past studies.

Therefore, this study aimed to ① assess the reuse potential of permeate water obtained in the dewatering of *S. obliquus* using microfiltration at both bench and pilot scales; ② evaluate the performance of the microfiltration dewatering process under various hydrodynamic conditions in a membrane bench-scale system in terms of cross-flow velocity (CFV) and trans-membrane pressure (TMP), through response surface methodology (RSM) [35,36]; and ③ investigate mechanisms that are crucial for the understanding and upscaling of any reuse approach, including biomass health status, cake layer compaction, operational scale, experimental protocol, and micronutrient reintegration in the reused water.

2. Materials and methods

2.1. Microalgae cultivation in the photobioreactor

S. obliquus (SAG 276-3b) microalgae were cultivated in a medium-size non-commercial photobioreactor, which grew microalgae suspensions until a concentration of approximately 1 $g{\cdot}L^{-1}$ was reached. The experimental photobioreactor and its hydraulic principle were described by Carone et al. [37]. This algal species is characterized by an elongated circular shape with an average diameter of roughly 10 μm. To evaluate the biomass concentration, dry-weight measurements were performed by filtering the suspension using glass microfiber filters with a pore size of 1.5 μm and then using a thermal scale operating at 120 °C for 10 min to eliminate the remaining moisture content.

The blue green-11 (BG-11) medium was used for biomass cultivation (Table S1 in Appendix A). The growth rate of the biomass in the BG-11 was used as a benchmark for comparing the growth rates of *S. obliquus* in the reused permeate solutions collected during the membrane filtration process.

The health state of the initial cultivated biomass (feed stream) was assessed using a multi-parameter approach on two different feed stream samples. One stream was cultivated in optimal conditions, while the second was cultivated in a liquid substrate with a temperature above 30 °C, slightly outside of its optimal range. The evaluation parameters included cell size distribution analyses, optical microscope images obtained in fluorescence mode, and comparisons to microalgae growth rates in the standard medium BG-11. A dependable, albeit qualitative, evaluation of the health of algae biomass in the feed streams was achieved based on the combined results of these assessment parameters.

2.2. Microfiltration setups and testing protocols

Microfiltration experiments were performed with a cross-flow bench-scale system and a cross-flow pilot-scale (one module) system. Both systems were built according to a standard configuration, including an inverter-controlled volumetric pump, a thermally insulated feed tank, and a tubular membrane housing module. The filtration tests were conducted with an initial feed suspension volume of 3 and 100 L for bench-scale and pilot-scale systems, respectively, and an initial microalgae concentration of 1 $g{\cdot}L^{-1}$. The two test parameters, namely, CFV and TMP, were set independently. The selected range for pressure is suitable for most microfiltration processes (~1–3 bar, 1 bar = 10^5 Pa), while the selected investigation range for CFV was about 1.0–3.5 $m{\cdot}s^{-1}$. Values of CFV between 0.5 and 4.0 $m{\cdot}s^{-1}$ have been commonly used in past studies, and consideration was given to the possibility that an increased CFV could affect cell integrity and the transmission of algae organic matter (AOM) across the membrane [38,39]. In both the bench-scale and pilot-scale systems, the water flux was measured continuously by monitoring the change in weight of the filtered solution, which was collected in a tank placed on a computer-interfaced balance, with weight measurements taken every 3 min (Fig. S1 in Appendix A).

We chose TiO_2-based ceramic membranes with a nominal pore size of 0.14 μm in their active layer for this application, as they have shown the best performance among various microfiltration and ultrafiltration membranes in the filtration of *S. obliquus* suspensions for algae harvesting [16]. These membranes were purchased from TAMI industries (France) and were characterized by 250 mm (47.1 cm^2 active filtration area) and 1170 mm (0.21 m^2 filtration area) lengths for the bench-scale and pilot-scale systems, respectively. To restore the initial characteristics of the membranes for each new experimental test, extensive membrane cleaning (both physical and chemical) was performed after each filtration process in two steps: ① quick flushing with deionized water to rinse the filtration unit and remove the remaining algal matter, followed by 30 min of continuous operation with deionized water, and ② 10 h of operation in backwash mode at a TMP of 2 bar, using a solution containing NaClO (6 $mL{\cdot}L^{-1}$) and citric acid (1.5 $g{\cdot}L^{-1}$). This last step was performed at a constant temperature of 50 °C reached by immersing a coil, which was heated by a thermostatic bath, in the cleaning solution tank. The aim of such extensive cleaning was solely to restore the initial membrane conditions to allow a fair comparison between tests run under different conditions; the cleaning protocol was not meant as a blueprint for actual operation practices.

Two filtration testing protocols were performed in batch mode for both the bench-scale and pilot-scale experiments. In the first protocol, the permeated water was collected continuously: the batch systems were operated in an open loop, namely, the permeate stream was collected in the external tank while the feed

solution was continuously concentrated. In the second protocol, steady-state flux conditions were reached before each collection phase: the batch systems were operated in a closed loop until a near constant flux was achieved, and at this point, the loop was opened to collect a portion of the water in the feed tank. The latter protocol was repeated for five different recovery values: 0, 25%, 50%, 75%, and 90%, corresponding to biomass concentrations in the feed tank of 1.00, 1.33, 2.00, 4.00, and 10.00 $g{\cdot}L^{-1}$, respectively, see Fig. S2 in Appendix A for further details.

2.3. Analysis of microfiltration productivity

Design-Expert (Stat-Ease Inc., USA) software was used to deploy the RSM model. The productivity of the filtration process was evaluated as a function of CFV and TMP. A central composite design was applied to define the number of experiments (i.e., conditions) required to optimize the variables and responses. Near steady-state permeate fluxes were recorded for each combination of CFV and TMP to build the response surface (experiments are listed in Table S2 and represented graphically in Fig. S3 in Appendix A). Thus, the resulting design is a regular two-level factorial design with two replicates (central points). See Section S1 in Appendix A for further details on the central composite design methodology. Alongside the RSM, pressure losses due to friction developing inside the filtration module were estimated for each value of CFV. This assessment was based on the Darcy–Weisbach equation (see Section S2 in Appendix A for details).

2.4. Evaluation of permeate quality and microfiltration rejection performance

Overall system rejection (R_{sys}) was calculated as $1-(C_{permeate,fin}/C_{feed,in})$, where $C_{permeate,fin}$ and $C_{feed,in}$ represent the concentration of a specific compound in the total permeate volume collected at the end of each test and its concentration in the initial feed suspension, respectively. Instantaneous membrane rejection (R_{mem}) was calculated as $1-(C_{permeate,t}/C_{feed,t})$, where $C_{permeate,t}$ and $C_{feed,t}$ represent the concentration of a compound in the permeate stream at a specific value of time *(t)* during the experiment and its concentration in the feed suspension at the same time value, respectively. Algal cell count, AOM concentration, and macro- and micro-nutrient rejection rates were analyzed. Dissolved organic carbon (DOC) was used as a proxy for AOM concentration, and it was measured with a total organic carbon (TOC) analyzer LCSH FA (Shimadzu, Italy; catalytic oxidation on Pt at 680 °C). Samples (40 mL) were collected and then filtered through 0.45 μm filters prior to analyses in the non-purgeable organic carbon mode, preceded by appropriate calibration. Specifically, DOC measurements were performed on the final permeate volume during the membrane filtration process at time intervals of approximately 30 min to evaluate the variation in permeate quality over time during the experiments. Furthermore, microscope fluorescence images were used to count and quantify the number of algae cells in the initial feed, concentrated feed, and permeate water. In terms of macronutrients and micronutrients, NO_3^-, Fe, Mn, Mg, and Ca were assessed because they have been determined to be the main requirements for appropriate microalgae growth and cultivation [40–43]. Ionic concentrations were measured with a Metrohm Eco ion chromatography system (Switzerland), while trace elements (Fe, Mn, and Mg) were detected using an inductively coupled plasma mass spectrometer (Perkin Elmer Optima 2000 DV, USA). Electrical conductivity (EC) measurements were performed using a CON 6+ portable conductivity meter (Oakton Instruments, USA).

2.5. Assessment of water reuse potential

To effectively reuse the permeate water as a medium for microalgae growth, macro- and micro-nutrients were reintegrated in the permeate solution in some tests to achieve the same concentrations as those of the ideal medium, BG-11. Target ion concentrations were reached by adding specific salts purchased from Carlo Erba (Italy). The growth of microalgae in the permeate water was conducted in the same non-commercial photobioreactor as that used to grow the initial feed microalgae suspensions. The growth tests were conducted for ten days, during which time biomass growth was monitored through dry weight concentration measurements. The increase in dry weight over time was used as a proxy for microalgae growth, and the recorded data points were fitted with linear regression curves (only when the value of the coefficient of determination (R^2) was higher than 95%). This protocol allowed for the comparison of growth tests performed in the ideal medium with those performed in the reused permeate with and without nutrient reintegration.

3. Results and discussion

3.1. Influence of initial biomass health status on microfiltration performance and permeate quality

The health status of the *S. obliquus* cultures cultivated in a pilot-scale photobioreactor was critically assessed before harvesting. Since no standard protocol exists to evaluate biomass health, multiple combined indicators were used in this study [44,45]. The indicators were assessed against the membrane filtration performance and the permeate quality to identify a possible relationship and to obtain conclusions that may be consequential for microalgae harvesting processes in general. Representative fluorescence microscope images and particle size distributions of *S. obliquus* cells from two relevant suspensions are shown in Fig. 1(a). Microscopy (Fig. 1(a)) revealed a noticeable difference between the two feed stream samples: the left-hand image (referred to as “healthy”) shows a substantially lower number of broken algae cells when compared to the right-hand image (referred to as “unhealthy”). The unhealthy culture presented a greater number of small particles (diameter < 5 μm) and a tendency for cell material to aggregate into large particles (diameter > 10 μm) compared to the healthy sample. This difference is attributed to the fact that low-quality algae cultures are typically characterized by weaker cell membranes that are more prone to damage [44]. Fig. 1(b) presents the growth rate of the two feed biomass streams in the pre-filtration phase (i.e., in the photobioreactor). The evolution of dry weight over time indicated that the unhealthy stream was associated with a biomass growth rate that was substantially lower than that of the healthy culture. More specifically, the concentration of the unhealthy culture did not exceed 1.5 $g{\cdot}L^{-1}$, while that of the healthy culture reached a value above 2.5 $g{\cdot}L^{-1}$ after eight days of cultivation.

To assess the performance and permeate quality of streams characterized by different health statuses, the two samples were separately used as feed suspensions in a bench-scale microfiltration system. Membrane filtration results are shown (Fig. 2(a)) for each of the two feed streams as the average of triplicate tests. For each test, pure water fluxes were measured before filtering the algal biomass streams to assess the integrity of the 0.14 μm TiO_2 membrane. Fig. 2(a) presents a clear difference in the flux trend, suggesting that the feed biomass quality strongly influences the filtration process performance. Furthermore, the pseudo steady-state value of permeate flux measured in the tests starting with healthy feed was consistently higher than the flux value

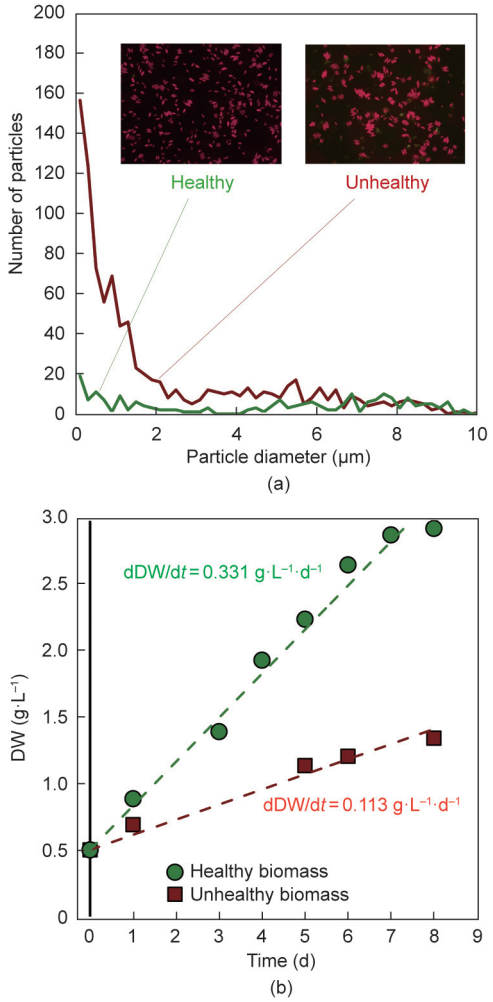

Fig. 1. Semi-quantitative assessment of biomass health state. (a) Representative fluorescence microscopy images of healthy and unhealthy biomass and particle size distribution: unhealthy biomass is characterized by a greater number of smaller particles (diameter < 5 μm). (b) Growth rates of microalgae in the photobioreactor before the dewatering process. Growth rates were estimated through dry-weight measurements. Three dry weight (DW) measurements were performed for each reported point: the relative average values are shown for the healthy biomass (green circles) and unhealthy biomass (red squares); standard deviation was always < 5%.

reached with unhealthy feed. Moreover, the profile related to the unhealthy feed was characterized by a faster initial drop. This phenomenon may be attributable to the larger number of small particles, consistent with Fig. 1(a), which may be responsible for faster clogging of the membrane surface pores. It has been widely documented that feed streams involving wide particle size distributions accelerate the fouling process and cake layer formation [46,47]. Moreover, since the cell membranes of unhealthy algae are considerably weaker, the release of inner cell substances, such as AOM, is likely facilitated. These compounds, as discussed by Zhang et al. [48] and Chiou et al. [49], represent a major issue for the filtration process as they promote the formation and growth of the cake layer [21,44].

Additionally, differences in permeate water quality were observed (Fig. 2(a) upper right corner). The permeate solution obtained when starting with an unhealthy feed was characterized by being yellow, while the permeate solution resulting from the healthy feed was transparent. This result aligns with the higher AOM concentration expected for the former stream to penetrate through the membrane pores [50,51]. The visual difference was corroborated by DOC analysis. The feed suspension with unhealthy biomass presented a DOC content four times higher than that of the healthy sample, while the respective permeate was characterized by a DOC content two times higher than that derived from healthy biomass filtration (Fig. 2(b)). Lastly, the spectrophotometric analysis further underlined the difference in the two permeates in terms of absorbance (Fig. 2(c)) and revealed a consistent and replicable difference in absorbance in the ultraviolet range (from 190 to 400 μm), with the permeate solution from unhealthy samples showing higher values than that from healthy samples.

In summary, the proposed algae health evaluation protocol effectively distinguished healthy from unhealthy biomass. Furthermore, *S. obliquus* streams characterized by different health statuses showed different productivity and permeate quality behaviors when filtered through a 0.14 μm TiO_2 membrane. These results may be partly responsible for the apparent discrepancies in filtration results reported in the literature when harvesting similar strains and using similar membrane-based processes. Notably, there is a continuum of health statuses, from very healthy to very unhealthy, and filtration performance may correlate with the specific health level within the spectrum. Furthermore, the evaluation results strongly suggest that biomass health is critical not only for the utilization of the algal product (e.g., extraction of valuable resources or optimized capture of CO_2), but also to guarantee the effective harvesting of algae and the sustainable processing of water for reuse following membrane filtration. Hereafter, results refer only to the use of healthy biomass.

3.2. Influence of hydrodynamic conditions on filtration process productivity

The influence of CFV and TMP on the performance of the filtration process was analyzed to identify the ideal balance of water flux and energy requirements. Experiments were designed using RSM in a central composite design, which provided a list of ten experiments, each involving a different combination of CFV and TMP values. The results (Fig. 3(a)) report the permeate water fluxes as a function of time using a bench-scale system. In all the experiments, when the *S. obliquus* feed replaced the pure water feed (time zero), the permeate flux showed an immediate flux drop. After this step, the flux continuously decreased for the first 30 min of filtration. This trend was aligned with the results of previous studies and was likely due to the development of a microalgae-rich cake layer at the surface of the membrane or within its active layer during the initial filtration stage [16,52,53]. Following this phase, the flux reached a near-stable value, showing a slow, steady decline, mostly due to the increasing concentration of the feed suspension with time. Notably, microscope images of the initial and final suspensions reflect the tendency of *S. obliquus* to form an increasing number of coenobia with increasing feed concentration, which likely further exacerbated fouling during filtration under all tested conditions (Fig. S4 in Appendix A) [54]. The values of pseudo steady-state flux reached toward the end of each test were used as input data to generate the model function, representing the productivity response of the RSM model. The flux value surface elaborated by the statistical model is thus presented as a function of CFV and TMP in Fig. 3(b). The related diagnostic plots are reported in Fig. S5 in Appendix A, while their description, which is supported by the findings of previous studies [55–58], is reported in detail in Section S1.

The results shown in Fig. 3(b) suggest that engineering optimization of the system is possible in terms of productivity and energy trade-offs. Notably, the model outcome indicates that below a CFV of approximately 1.5 $m \cdot s^{-1}$, an increase in TMP translates into a decrease in productivity. A similar trend was observed by Sun et al. [59] during the microfiltration of *Chlorella vulgaris*, and the effect was attributed to the presence of polysaccharides and other foulants, which can be densely compacted even at low

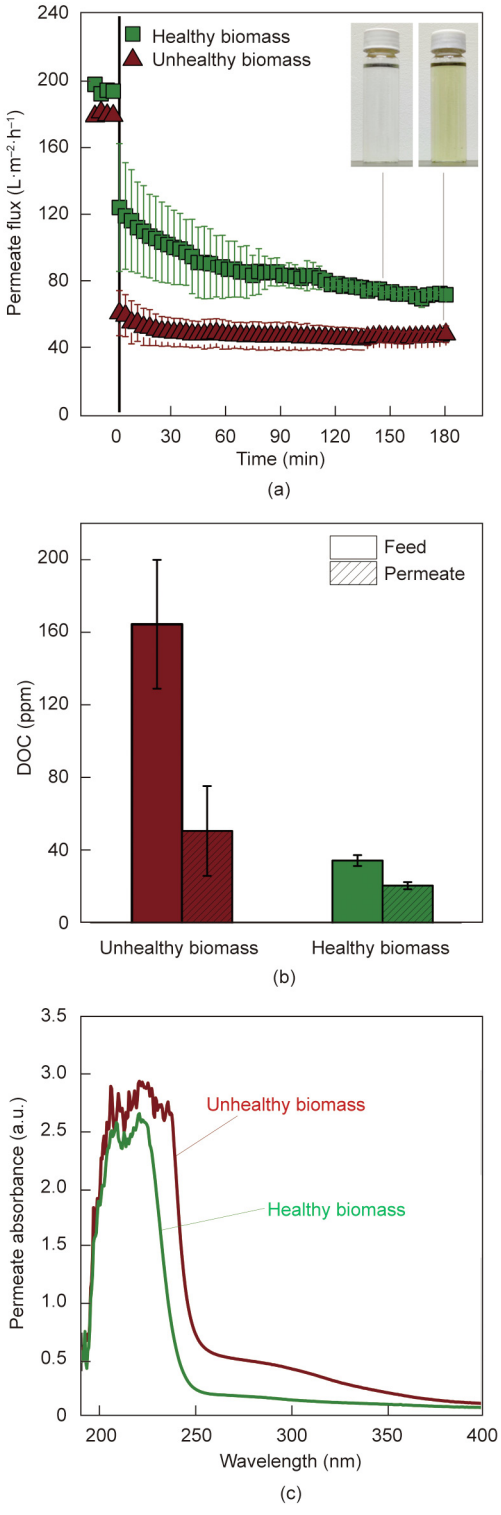

Fig. 2. Results of microfiltration tests obtained from suspensions containing biomass of different health status. (a) Comparison of flux behavior: permeate flux was calculated as an average between triplicate tests; bars indicate the related standard deviation for each data point. The tests were performed at an applied feed pressure of 1 bar and with a CFV of 2 $m \cdot s^{-1}$. The photographs in the right upper corner present the color difference between the two permeate solutions. (b) Difference in DOC content between solutions related to tests performed with healthy and unhealthy biomass feed and permeate solutions. (c) Ultraviolet absorbance of the permeate solutions obtained starting from healthy and unhealthy biomass feed suspensions. ppm: parts per million; a.u.: arbitrary unit.

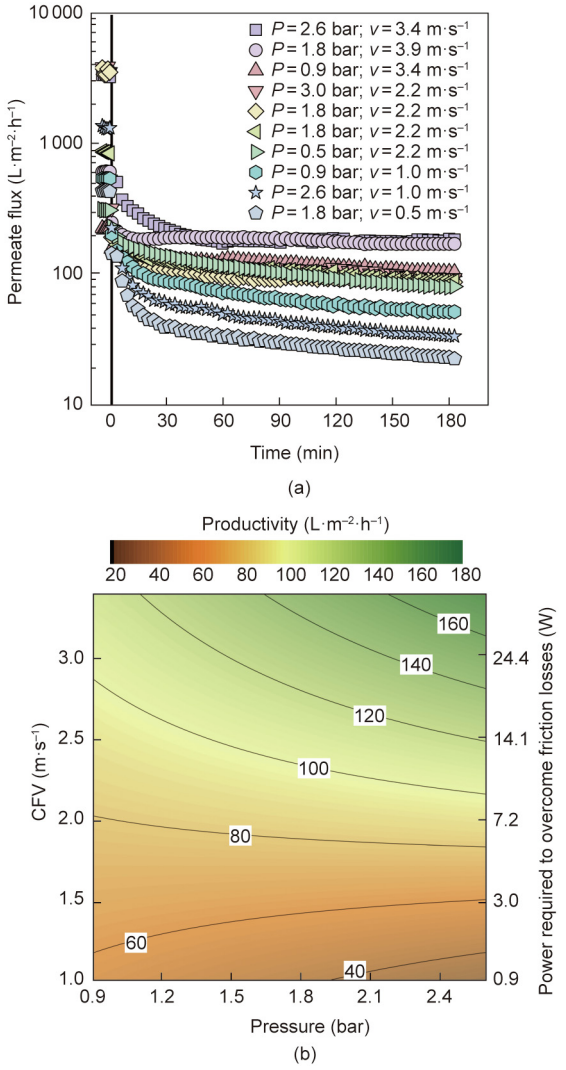

Fig. 3. Results of the ten different tests designed using the RSM model in central composite design to evaluate the flux behavior and the friction losses under different conditions of transmembrane pressure (P) and CFV (v). (a) Experimental results of the flux tests performed with each combination of hydrodynamic conditions. (b) The near steady-state fluxes from the profiles were then applied to build the model function. Here, the right axis represents the power needed to overcome the pressure loss due to the friction along a 1 m long membrane module (Fig. S6 in Appendix A).

operating pressure, thus limiting productivity [60,61]. However, If the CFV is maintained above the threshold of 1.5 $m \cdot s^{-1}$, the model suggests that the tangential forces are sufficiently high to counteract the compaction effect on the cake layer caused by the TMP. Indeed, above the threshold CFV, an increase in TMP produces an incremental increase in productivity.

The above results imply that the value of CFV should be kept as high as possible. However, working at high CFV values would result in considerable energy losses and increased power requirements. In addition, high CFV values may lead to possible damage to the algae cells due to excessive shear stress, with consequent impairment of both the biomass and permeate quality [39,62]. The right axis in Fig. 3(b) represents the estimated power needed to overcome friction losses associated with each value of CFV. The equations used to estimate the power requirements are

detailed in Section S2. The ideal balance between productivity and power was then identified from the plot of power vs CFV (Fig. S6 in Appendix A). For this specific system, a CFV of 2.4 $m \cdot s^{-1}$ may be assumed to be a suitable compromise. At 2.4 $m \cdot s^{-1}$ CFV, the response surface indicates that increasing the TMP above roughly 1.4 bar would not allow any further benefit in terms of productivity (Fig. 3(b)), as the contour iso-flux lines are nearly horizontal beyond this value.

Therefore, the optimized conditions may be identified as a TMP of 1.4 bar and a CFV of 2.4 $m \cdot s^{-1}$ for harvesting the *S. obliquus* feed under the pilot-scale microfiltration conditions investigated in this study. In summary, the experimental modeling approach facilitated the preliminary optimization of filtration performance and supported a reasonable estimation of the expected flux values for every chosen combination of CFV and TMP.

3.3. Filtration process scale-up: Evaluation of productivity, permeate quality, and testing protocols

Previous studies have mainly been performed at the bench scale without assessing the validity of the results at larger scales. However, discrepancies exist among the results obtained at different scales in the applications of microalgae harvesting. Therefore, comparing bench- and pilot-scale configurations in this study will provide a valuable reference. In both bench- and pilot-scale systems, healthy biomass was filtered under the selected conditions of CFV and TMP (2.4 $m \cdot s^{-1}$ and 1.4 bar, respectively). The permeate flux results, both in continuous and steady-state permeate collection modes, are shown in Fig. 4. Under continuous operation, the permeate flux achieved using the bench-scale rig (Fig. 4(a)) was consistently lower than that observed under pilot-scale operation (Fig. 4(b)). This result may be explained by the different filtration times required to achieve the same recovery rate at two different scales, which were larger for bench-scale experiments than for pilot-scale experiments. Foulants have more time to be deposited in bench-scale operations than pilot-scale operations for any recovery value. Specifically, the tests with the pilot-scale rig reached a 90% recovery rate in approximately 6 h, while the bench-scale system required nearly double that amount of time to achieve the same result under identical operating conditions (Fig. S7 in Appendix A). Although this result is logical, it is hardly accounted for in investigations reported in the literature. Moreover, this result indicates that the specific configuration and scale of the filtration systems have an important influence on the filtration results, thus adding an additional variable that complicates direct comparisons between different studies.

To allow a fair comparison of the filtration performance while neglecting the time influence, a second testing protocol was exploited, where the productivity was measured under near steady-state conditions at discretized recovery steps, for both bench- and pilot-scale operations (Fig. 4). To reach a stable flux condition in the pilot-scale experiments, approximately 9 h (Fig. S7) were required, a timeframe that is consistent with those determined in previous research [63,64]. Overall, even under near steady-state conditions, the observed flux was consistently lower with the bench-scale system compared to that under the pilot-scale system. These results highlight the key role of scale-specific effects when productivity assessment is the target of the investigation. While the bench scale system allows a conservative estimation of productivity, the pilot-scale rig may be more representative of real-scale operations, as the flux profiles obtained with the different testing protocols (continuous and stable flux) were similar, as opposed to those observed with the smaller bench-scale rig. This result may be attributed to the more representative and suitable hydrodynamic conditions inside the pilot-scale membrane module, which translated into lower foulant deposition and faster achievement of equilibrium conditions compared to those of the small-scale module. Furthermore, as previously mentioned, *S. obliquus* algae tend to form coenobia, whose number correlates with cell concentration (Fig. S4). Algae clusters were more constrained in the lab-scale module; specifically, almost 7.4 times more constrained according to the transversal channel areas of the two modules, which may have further exacerbated fouling. Further investigations are required to corroborate these results and validate this hypothesis.

The permeate quality was assessed during and at the end of the pilot-scale filtration experiments. DOC and EC were used as proxies for AOM and ionic concentration during filtration [51,65]. Results

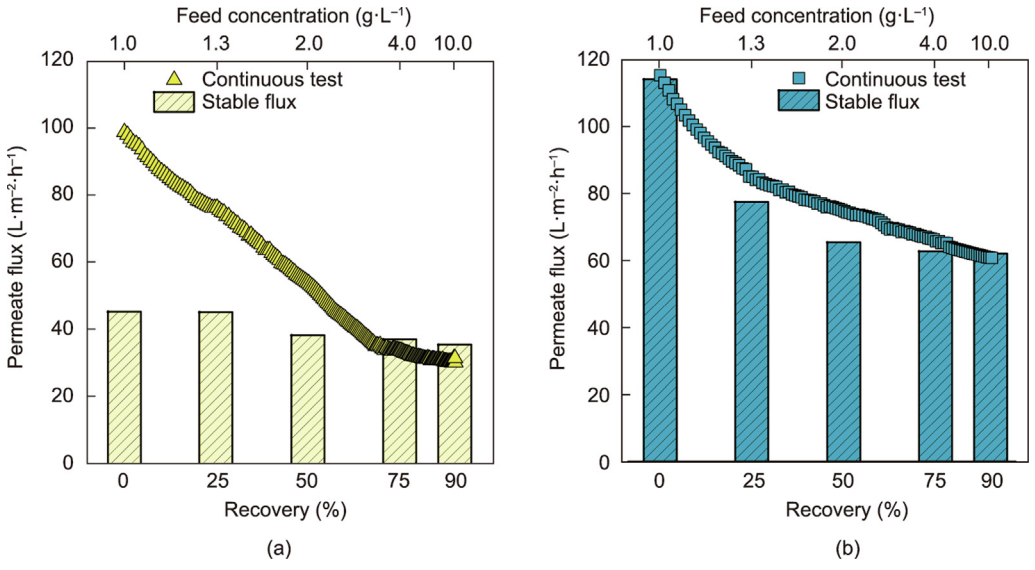

Fig. 4. Analysis of process scale-up behavior and influence of testing protocols. Permeate flux data are reported as a function of recovery values. Bars represent the flux measured upon reaching stabilization at specific recovery values, while data points refer to a test performed with continuous permeate collection (open loop) until a recovery of 90% was reached. (a, b) Tubular 0.14 μm ceramic TiO_2 membranes were used for all tests, with an effective membrane area of (a) 47.1 cm^2 for the bench-scale rig and (b) 0.21 m^2 for the pilot-scale rig. For additional details on the testing protocols, please see Fig. S2. A time solved analysis of the tests is reported in Fig. S7 in Appendix A). Prior to each dewatering experiment, similar pure water fluxes of 650 and 680 $L \cdot m^{-2} \cdot h^{-1}$ were measured for the membranes used in the bench-scale and the pilot-scale systems, respectively. Note that 0 recovery indicates that only the water needed for the measurement of the flux was collected.

are shown in Fig. 5(a), where a linear increase in DOC concentration in the permeate stream as a function of time can be observed. This increment translated into a deterioration in the overall permeate quality during the test. Specifically, DOC rejection (R_{mem}) decreased from 76% to 55% between the initial and final stages of filtration, namely, at 90% recovery. The reduction in rejection caused by fouling in organic substance filtration was also reported by Schäfer et al. [66], who showed how the fouling phenomenon can either increase or decrease rejection depending on the selectivity of the fouling layer. For this specific application, the gradual deterioration of the permeate quality may also be associated with the development of a biofouling layer on the membrane active surface, in which microorganisms accumulate and grow while producing metabolic products. It has been reported that biofouling layers produce low molecular weight AOM that can diffuse through the membrane pores [67]. Moreover, algae are continuously subjected to considerable shear stress during the test, which may cause extensive damage to the cell walls and consequent AOM release [44,68]. However, EC values were stable between 900 and 1000 $\mu S \cdot cm^{-1}$ throughout the entirety of the test duration, thus suggesting a stable concentration of nutrients and other ions in the collected permeate. Overall, the permeate quality data were consistent with the lab-scale results obtained in previous investigations that involved filtering the same algal strain with the same pore-size membrane, thus supporting the reliability of this analysis [16].

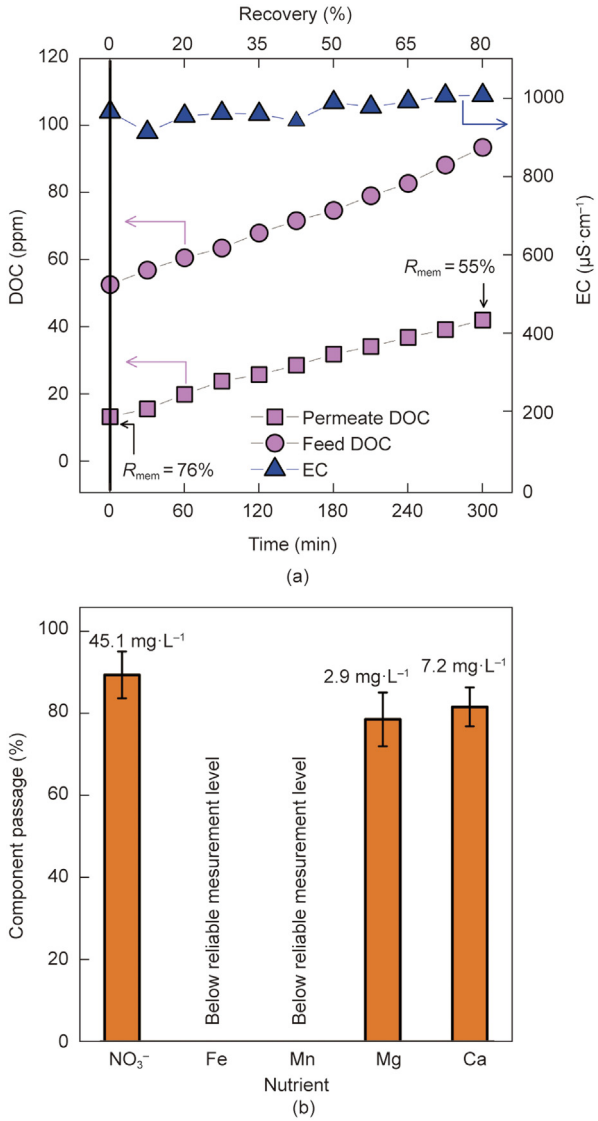

Fig. 5. Permeate quality and water flux profiles from pilot-scale experimentation. (a) Evolution of feed and permeate DOC and EC over time. Data were collected every 30 min. R_{mem} are also specified for the first and last DOC data. Lines connecting the data points are intended only as a guide for the eye. (b) Passage of various compounds was obtained as the ratio between the final compound concentration in the total collected permeate solution and the compound concentration in the initial feed suspension (%). Results are reported as average from three replicate tests and with the related standard deviation values. The labels over each column represent the absolute ion concentrations in the final permeate solution. Concentration values were then used to calculate the amount of nutrients to be reintegrated to meet the ideal medium (BG-11) concentration values, with the final aim of reusing the effluent.

At the end of the filtration run, the nutrient composition of the permeate was analyzed in detail, allowing for the evaluation of the overall passages of NO_3^-, Fe, Mn, Mg, and Ca. High passage rates were measured for NO_3^-, Mg, and Ca (89%, 78%, and 81%, respectively; Fig. 5(b)). Notably, these ions play an important role in microalgae growth [40–43]. This positive result reflects the effectiveness of the membrane selectivity in rejecting the algae cells and organic matter while allowing the passage of nutrients. The concentration of nutrients in the total recovered permeate was then compared with that in the ideal medium (BG-11) to inform precise nutrient reintegration and restoration of the initial ideal conditions. Conservatively, Fe and Mn were fully reintegrated regardless of the real values of their concentrations in the permeate, which could not be measured as they were below the detection limits.

3.4. Permeate reuse potential: Regulating factors

After the reintegration of the main nutrients in the permeate water obtained from pilot-scale filtration of *S. obliquus*, the reuse potential of this solution was evaluated by using it as a new medium for the growth of *S. obliquus*. This assessment was performed through three different algae cultivation tests in a pilot-scale photobioreactor, each investigating a different permeate solution. Two out of three cultivation experiments were performed after complete nutrient reintegration, whereas the third test involved only the reintegration of NO_3^-, which is considered the most important nutrient for suitable microalgae growth [40]. Fig. 6 presents the results of this assessment in comparison to benchmark growth data obtained using the BG-11 medium. The highest growth rate observed when reusing water was 0.244 $g \cdot L^{-1} \cdot d^{-1}$, which is remarkably close to the ideal medium rate of 0.268 $g \cdot L^{-1} \cdot d^{-1}$. A slightly lower growth rate of 0.154 $g \cdot L^{-1} \cdot d^{-1}$ was observed in a replicate test, which is still within the acceptable range based on the results of previous studies [69,70]. The discrepancy between replicate results in this study may be considered acceptable owing to the many factors involved in the algae cultivation process; thus, the differences may not be due to a difference in permeate quality. Furthermore, when only NO_3^- was reintegrated, a sudden decline was observed following relatively fast growth in the first six days of the experiment. This result may be attributed to the consumption of the nutrients that had not been reintegrated after roughly six days of growth and highlights the importance of both macro- and micro-nutrient reintegration in permeate reuse. Additionally, the results of cell size distribution analysis (Fig. S8 in Appendix A) imply that suspensions that presented adequate growth rates were associated with narrow particle size distributions, namely, "healthy" biomass.

Overall, the results obtained with the pilot-scale filtration and photobioreactor systems were promising and consistent with the findings of previous studies [22,23]. However, further studies are required to investigate the behavior and limiting factors of a system undergoing several cycles of harvesting and reuse. Additionally, future research should consider the likely necessity of

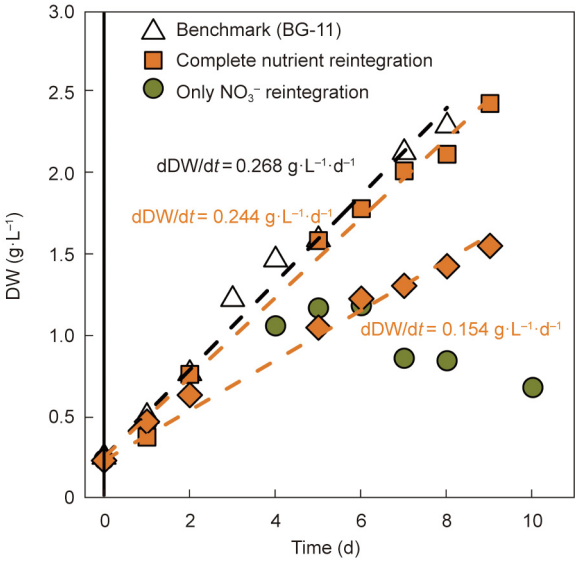

Fig. 6. Analysis of microalgae growth performance in the permeate solution collected from three pilot-scale tests under optimized conditions and comparison with the ideal medium (BG-11). Growth rates were estimated through dry weight measurements. Only linear fitting lines with R^2 values higher than 95% are reported. NO_3^- reintegration was performed in the test reported with green circles, while data series reported with orange squares (two replicates) are associated with tests performed following both macro- and micro-nutrient reintegration, such as NO_3^-, Ca, Fe, Mn, and Mg.

strategies involving mixing a fraction of the permeate stream with an ideal medium, such as, strategies involving less than 100% reuse, identifying the optimal mixing ratios, and/or the frequency of possible disposal and complete substitution of the cultivation water in case unwanted substances accumulate after repeated reuse cycles.

4. Conclusions

Ceramic microfiltration of the microalgae *S. obliquus* was investigated with a 0.14 μm TiO_2 membrane in terms of filtration performance and with the aim of reusing the permeate solution as a cultivation medium. The investigation was performed under both bench- and pilot-scale conditions. The influence of TMP and CFV on productivity was investigated, and the results suggested that the applied pressure increases productivity only when the CFV is maintained above a threshold (approximately 1.5 m·s^{-1}) that counterbalances the compaction of the cake layer and the tendency of *S. obliquus* to form coenobia. To achieve high productivity while minimizing the required pressure and the friction losses inside the membrane module, optimal conditions of 1.4 bar and 2.4 m·s^{-1} for TMP and CFV, respectively, were identified in the system investigated in this study. The membrane provided virtually complete algae rejection and suitable DOC rejection while allowing adequate nutrient passage (i.e., NO_3^-, Mg, and Ca) in the permeate solution. When the permeate solution was reused, the growth rate of new microalgae cultures showed promising results when both macro- and micronutrients were reintegrated.

Along with the experimental investigation, a series of challenges and optimization factors were highlighted, which may contribute to a greater understanding of discrepancies among previous studies and support rational scale-up efforts. First, the feed stream quality was found to play a substantial role in filtration; starting with a healthy biomass increased membrane productivity and permeate quality. A comparison of outcomes was performed between bench and pilot approaches and between different experimental protocols. The results obtained at the two scales or under different filtration modes were only partially comparable, implying the importance of scale effects and experimental practices. This finding may explain some inconsistencies in the literature. Notably, pilot-scale tests showed better and more robust performance compared to bench-scale experiments, which may be interpreted as a positive outcome for the potential of reuse strategies.

Overall, the results of this study suggest that membrane separation is an effective process for the first phase of microalgae dewatering (i.e., up to a feasible concentration factor) and for producing a high-quality permeate stream when operating under suitable conditions. Among the many future investigations that would support efforts aimed at water reuse in this field, the viability of direct integration of the membrane dewatering system with the cultivating photobioreactor should be studied under continuous operation. Moreover, targeted investigations are required to quantitatively assess the portion of permeate water that may be reused and to design a feasible in-line nutrient reintegration strategy.

Acknowledgments

This work was supported by the Politecnico di Torino and the CleanWaterCenter@PoliTo (58_DIM20TIRALB, 58_DIM22TIRALB, and 01_TRIN_CI_CWC).

Compliance with ethics guidelines

Marco Malaguti, Lorenzo Craveri, Francesco Ricceri, Vincenzo Riggio, Mariachiara Zanetti, and Alberto Tiraferri declare that they have no conflict of interest or financial conflicts to disclose.

Appendix A. Supplementary data

Supplementary data to this article can be found online at https://doi.org/10.1016/j.eng.2023.07.010.

References

[1] Spolaore P, Joannis-Cassan C, Duran E, Isambert A. Commercial applications of microalgae. J Biosci Bioeng 2006;101(2):87–96.
[2] Torres-Tiji Y, Fields FJ, Mayfield SP. Microalgae as a future food source. Biotechnol Adv 2020;41:107536.
[3] Draaisma RB, Wijffels RH, (Ellen) Slegers PM, Brentner LB, Roy A, Barbosa MJ. Food commodities from microalgae. Curr Opin Biotechnol 2013;24(2):169–77.
[4] Mourelle ML, Gómez CP, Legido JL. The potential use of marine microalgae and cyanobacteria in cosmetics and thalassotherapy. Cosmetics 2017;4(4):46.
[5] Morocho-Jácome AL, Ruscinc N, Martinez RM, de Carvalho JCM, Santos de Almeida T, Rosado C, et al. (Bio)Technological aspects of microalgae pigments for cosmetics. Appl Microbiol Biotechnol 2020;104(22):9513–22.
[6] Wollmann F, Dietze S, Ackermann JU, Bley T, Walther T, Steingroewer J, et al. Microalgae wastewater treatment: biological and technological approaches. Eng Life Sci 2019;19(12):860–71.
[7] Abdel-Raouf N, Al-Homaidan A, Ibraheem I. Microalgae and wastewater treatment. Saudi J Biol Sci 2012;19(3):257–75.
[8] Oncel SS. Microalgae for a macroenergy world. Renew Sustain Energy Rev 2013;26:241–64.
[9] Kumar A, Ergas S, Yuan X, Sahu A, Zhang Q, Dewulf J, et al. Enhanced CO_2 fixation and biofuel production via microalgae: recent developments and future directions. Trends Biotechnol 2010;28(7):371–80.
[10] Zeng X, Danquah MK, Chen XD, Lu Y. Microalgae bioengineering: from CO_2 fixation to biofuel production. Renew Sustain Energy Rev 2011;15(6):3252–60.
[11] Sharma KK, Garg S, Li Y, Malekizadeh A, Schenk PM. Critical analysis of current microalgae dewatering techniques. Biofuels 2013;4(4):397–407.
[12] Chen CY, Yeh KL, Aisyah R, Lee DJ, Chang JS. Cultivation, photobioreactor design and harvesting of microalgae for biodiesel production: a critical review. Bioresour Technol 2011;102(1):71–81.
[13] Mandal S, Mallick N. Microalga *Scenedesmus obliquus* as a potential source for biodiesel production. Appl Microbiol Biotechnol 2009;84(2):281–91.
[14] Ho SH, Chen WM, Chang JS. *Scenedesmus obliquus* CNW-N as a potential candidate for CO_2 mitigation and biodiesel production. Bioresour Technol 2010;101(22):8725–30.

[15] Martínez ME, Sánchez S, Jiménez J, El Yousfi F, Muñoz L. Nitrogen and phosphorus removal from urban wastewater by the microalga *Scenedesmus obliquus*. Bioresour Technol 2000;73(3):263–72.
[16] Ricceri F, Malaguti M, Derossi C, Zanetti M, Riggio V, Tiraferri A. Microalgae biomass concentration and reuse of water as new cultivation medium using ceramic membrane filtration. Chemosphere 2022;307:135724.
[17] Batan L, Quinn JC, Bradley TH. Analysis of water footprint of a photobioreactor microalgae biofuel production system from blue, green and lifecycle perspectives. Algal Res 2013;2(3):196–203.
[18] Suparmaniam U, Lam MK, Uemura Y, Lim JW, Lee KT, Shuit SH. Insights into the microalgae cultivation technology and harvesting process for biofuel production: a review. Renew Sustain Energy Rev 2019;115:109361.
[19] Barros AI, Gonçalves AL, Simões M, Pires JC. Harvesting techniques applied to microalgae: a review. Renew Sustain Energy Rev 2015;41:1489–500.
[20] Singh G, Patidar S. Microalgae harvesting techniques: a review. J Environ Manage 2018;217:499–508.
[21] Bilad M, Arafat HA, Vankelecom IF. Membrane technology in microalgae cultivation and harvesting: a review. Biotechnol Adv 2014;32(7):1283–300.
[22] Nędzarek A, Drost A, Harasimiuk F, Tórz A, Bonisławska M. Application of ceramic membranes for microalgal biomass accumulation and recovery of the permeate to be reused in algae cultivation. J Photochem Photobiol B Biol 2015;153:367–72.
[23] Discart V, Bilad M, Marbelia L, Vankelecom I. Impact of changes in broth composition on *Chlorella vulgaris* cultivation in a membrane photobioreactor (MPBR) with permeate recycle. Bioresour Technol 2014;152:321–8.
[24] Larronde-Larretche M, Jin X. Microalgae (*Scenedesmus obliquus*) dewatering using forward osmosis membrane: influence of draw solution chemistry. Algal Res 2016;15:1–8.
[25] Giagnorio M, Ricceri F, Tagliabue M, Zaninetta L, Tiraferri A. Hybrid forward osmosis–nanofiltration for wastewater reuse: system design. Membranes 2019;9(5):61.
[26] Hwang JH, Rittmann BE. Effect of permeate recycling and light intensity on growth kinetics of *Synechocystis* sp. PCC 6803. Algal Res 2017;27:170–6.
[27] Loftus SE, Johnson ZI. Reused cultivation water accumulates dissolved organic carbon and uniquely influences different marine microalgae. Front Bioeng Biotechnol 2019;7:101.
[28] Lu Z, Loftus S, Sha J, Wang W, Park MS, Zhang X, et al. Water reuse for sustainable microalgae cultivation: current knowledge and future directions. Resour Conserv Recycling 2020;161:104975.
[29] Sha J, Lu Z, Ye J, Wang G, Hu Q, Chen Y, et al. The inhibition effect of recycled *Scenedesmus acuminatus* culture media: influence of growth phase, inhibitor identification and removal. Algal Res 2019;42:101612.
[30] Wang X, Lin L, Lu H, Liu Z, Duan N, Dong T, et al. Microalgae cultivation and culture medium recycling by a two-stage cultivation system. Front Environ Sci Eng 2018;12(6):14.
[31] Fret J, Roef L, Diels L, Tavernier S, Vyverman W, Michiels M. Combining medium recirculation with alternating the microalga production strain: a laboratory and pilot scale cultivation test. Algal Res 2020;46:101763.
[32] Aditya L, Vu HP, Nguyen LN, Mahlia TMI, Hoang NB, Nghiem LD. Microalgae enrichment for biomass harvesting and water reuse by ceramic microfiltration membranes. J Membr Sci 2023;669:121287.
[33] Farooq W, Suh WI, Park MS, Yang JW. Water use and its recycling in microalgae cultivation for biofuel application. Bioresour Technol 2015;184:73–81.
[34] Wu M, Du M, Wu G, Lu F, Li J, Lei A, et al. Water reuse and growth inhibition mechanisms for cultivation of microalga *Euglena gracilis*. Biotechnol Biofuels 2021;14(1):132.
[35] Ricceri F, Blankert B, Ghaffour N, Vrouwenvelder JS, Tiraferri A, Fortunato L. Unraveling the role of feed temperature and cross-flow velocity on organic fouling in membrane distillation using response surface methodology. Desalination 2022;540:115971.
[36] Ricceri F, Farinelli G, Giagnorio M, Zamboi A, Tiraferri A. Optimization of physico-chemical and membrane filtration processes to remove high molecular weight polymers from produced water in enhanced oil recovery operations. J Environ Manage 2022;302:114015.
[37] Carone M, Alpe D, Costantino V, Derossi C, Occhipinti A, Zanetti M, et al. Design and characterization of a new pressurized flat panel photobioreactor for microalgae cultivation and CO_2 bio-fixation. Chemosphere 2022;307:135755.
[38] Bamba BSB, Tranchant CC, Ouattara A, Lozano P. Harvesting of microalgae biomass using ceramic microfiltration at high cross-flow velocity. Appl Biochem Biotechnol 2021;193(4):1147–69.
[39] Novoa AF, Vrouwenvelder JS, Fortunato L. Membrane fouling in algal separation processes: a review of influencing factors and mechanisms. Front Chem Eng 2021;3:687422.
[40] Sanz-Luque E, Chamizo-Ampudia A, Llamas A, Galvan A, Fernandez E. Understanding nitrate assimilation and its regulation in microalgae. Front Plant Sci 2015;6:899.
[41] Rana MS, Prajapati SK. Resolving the dilemma of iron bioavailability to microalgae for commercial sustenance. Algal Res 2021;59:102458.
[42] Liu J, Tan K, He L, Qiu Y, Tan W, Guo Y, et al. Effect of limitation of iron and manganese on microalgae growth in fresh water. Microbiology 2018;164(12):1514–21.
[43] Polat E, Yüksel E, Altınbaş M. Mutual effect of sodium and magnesium on the cultivation of microalgae *Auxenochlorella protothecoides*. Biomass Bioenergy 2020;132:105441.
[44] Elisabeth B, Rayen F, Behnam T. Microalgae culture quality indicators: a review. Crit Rev Biotechnol 2021;41(4):457–73.
[45] Chowdury KH, Nahar N, Deb UK. The growth factors involved in microalgae cultivation for biofuel production: a review. Comput Water Eng Environ Eng 2020;9(04):185–215.
[46] Malaguti M, Novoa AF, Ricceri F, Giagnorio M, Vrouwenvelder JS, Tiraferri A, et al. Control strategies against algal fouling in membrane processes applied for microalgae biomass harvesting. J Water Process Eng 2022;47:102787.
[47] Marbelia L, Mulier M, Vandamme D, Muylaert K, Szymczyk A, Vankelecom IFJ. Polyacrylonitrile membranes for microalgae filtration: influence of porosity, surface charge and microalgae species on membrane fouling. Algal Res 2016;19:128–37.
[48] Zhang X, Fan L, Roddick FA. Influence of the characteristics of soluble algal organic matter released from *Microcystis aeruginosa* on the fouling of a ceramic microfiltration membrane. J Membr Sci 2013;425–6:23–9.
[49] Chiou YT, Hsieh ML, Yeh HH. Effect of algal extracellular polymer substances on UF membrane fouling. Desalination 2010;250(2):648–52.
[50] Ghernaout D, Elboughdiri N, Ghareba S, Salih A. Coagulation process for removing algae and algal organic matter—an overview. Open Access Libr 2020;7(04):1–21.
[51] Villacorte LO, Ekowati Y, Neu TR, Kleijn JM, Winters H, Amy G, et al. Characterisation of algal organic matter produced by bloom-forming marine and freshwater algae. Water Res 2015;73:216–30.
[52] Zhang X, Hu Q, Sommerfeld M, Puruhito E, Chen Y. Harvesting algal biomass for biofuels using ultrafiltration membranes. Bioresour Technol 2010;101(14):5297–304.
[53] Nędzarek A, Mitkowski PT. The fouling effect on commercial ceramic membranes during filtration of microalgae *Chlorella vulgaris* and *Monoraphidium contortum*. Energies 2022;15(10):3745.
[54] Oliveira CYB, Oliveira CDL, Prasad R, Ong HC, Araujo ES, Shabnam N, et al. A multidisciplinary review of *Tetradesmus obliquus*: a microalga suitable for large-scale biomass production and emerging environmental applications. Rev Aquacult 2021;13(3):1594–618.
[55] Pashaei H, Ghaemi A, Nasiri M, Karami B. Experimental modeling and optimization of CO_2 absorption into piperazine solutions using RSM-CCD methodology. ACS Omega 2020;5(15):8432–48.
[56] Mason RL, Gunst RF, Hess JL. Statistical design and analysis of experiments: with applications to engineering and science. New Jersey: John Wiley & Sons; 2003.
[57] Noordin MY, Venkatesh V, Sharif S, Elting S, Abdullah A. Application of response surface methodology in describing the performance of coated carbide tools when turning AISI 1045 steel. J Mater Process Technol 2004;145(1):46–58.
[58] Ahmadi M, Vahabzadeh F, Bonakdarpour B, Mofarrah E, Mehranian M. Application of the central composite design and response surface methodology to the advanced treatment of olive oil processing wastewater using Fenton's peroxidation. J Hazard Mater 2005;123(1–3):187–95.
[59] Sun X, Wang C, Tong Y, Wang W, Wei J. A comparative study of microfiltration and ultrafiltration for algae harvesting. Algal Res 2013;2(4):437–44.
[60] Krstić DM, Markov SL, Tekić MN. Membrane fouling during cross-flow microfiltration of *Polyporus squamosus* fermentation broth. Biochem Eng J 2001;9(2):103–9.
[61] Rossi N, Derouiniot-Chaplain M, Jaouen P, Legentilhomme P, Petit I. Arthrospira platensis harvesting with membranes: fouling phenomenon with limiting and critical flux. Bioresour Technol 2008;99(14):6162–7.
[62] Bamba BS, Lozano P, Ouattara A, Elcik H. Pilot-scale microalgae harvesting with ceramic microfiltration modules: evaluating the effect of operational parameters and membrane configuration on filtration performance and membrane fouling. J Chem Technol Biotechnol 2021;96(3):603–12.
[63] Gerardo ML, Oatley-Radcliffe DL, Lovitt RW. Minimizing the energy requirement of dewatering *Scenedesmus* sp. by microfiltration: performance, costs, and feasibility. Environ Sci Tech 2014;48(1):845–53.
[64] Gerardo ML, Zanain MA, Lovitt RW. Pilot-scale cross-flow microfiltration of Chlorella minutissima: a theoretical assessment of the operational parameters on energy consumption. J Chem Eng 2015;280:505–13.
[65] Mostafa SS, Shalaby EA, Mahmoud GI. Cultivating microalgae in domestic wastewater for biodiesel production. Not Sci Biol 2012;4(1):56–65.
[66] Schäfer A, Fane AG, Waite T. Fouling effects on rejection in the membrane filtration of natural waters. Desalination 2000;131(1–3):215–24.
[67] Fortunato L, Jeong S, Leiknes T. Time-resolved monitoring of biofouling development on a flat sheet membrane using optical coherence tomography. Sci Rep 2017;7(1):15.
[68] Wang C, Lan CQ. Effects of shear stress on microalgae-a review. Biotechnol Adv 2018;36(4):986–1002.
[69] de Morais MG, Costa JAV. Biofixation of carbon dioxide by *Spirulina* sp. and *Scenedesmus obliquus* cultivated in a three-stage serial tubular photobioreactor. J Biotechnol 2007;129(3):439–45.
[70] Liao Q, Li L, Chen R, Zhu X. A novel photobioreactor generating the light/dark cycle to improve microalgae cultivation. Bioresour Technol 2014;161:186–91.